

Juan J. Aristizabal-Henao<sup>1</sup>, Sylwia Stopka<sup>1</sup>, Stephane Gesta<sup>1</sup>, Devon Van Cura<sup>1</sup>, Srada Karmacharya<sup>1</sup>, Megan K. Cox<sup>1</sup>, Alba Pesini<sup>2</sup>, Eliana Barriocanal Casado<sup>2</sup>, Catarina M. Quinzii<sup>2</sup>, Vijay Modur<sup>1</sup>, Niven R. Narain<sup>1,3</sup>, Michael A. Kiebish<sup>1</sup>,  
<sup>1</sup>BPGbio Inc., Framingham, MA, 01701, <sup>2</sup>Department of Neurology Columbia University Medical Center, New York, NY, 10032 <sup>3</sup>Department of Molecular Biology and Department of Dermatology and Cutaneous Surgery, University of Miami Miller School of Medicine, Miami, FL 33136

## INTRODUCTION & METHODS

### Introduction

Coenzyme Q10 (CoQ10) is vital for mitochondrial function, playing a central role in cellular bioenergetics and membrane fluidity. Dysregulated CoQ10 metabolism contributes to mitochondrial diseases and deficiency syndromes, yet the mechanisms remain poorly understood. To address this, we developed a novel LC-MS/MS and MALDI-MSI quinomics workflow to profile CoQ10 and related metabolites comprehensively. Using this platform, we examined a lipid nanoparticle CoQ10 formulation (BPM31510) in a CoQ-deficient mouse model (COQ4KI), uncovering novel aspects of quinone regulation, metabolic regulation, and potential therapeutic strategies for mitochondrial diseases.

### Methods

COQ4-deficient mice were administered BPM31510 (200 mg/kg CoQ10) via intraperitoneal injection every other day over two weeks. At termination, kidney, liver, brain, muscle, heart, adipose, and ear (skin) tissues were harvested. Quinones were extracted from tissue homogenates using isopropanol and deuterium-labeled CoQ10 as an internal standard. Samples were analyzed by HPLC-MS/MS on an Agilent LC with a Waters Acquity HSS-T3 column, a binary multi-step gradient, and a Thermo Q-Exactive Plus mass spectrometer. Data were acquired using scheduled parallel reaction monitoring (PRM) to semi-quantify ~30 quinones. Absolute quantification of oxidized CoQ10 was done using isotope dilution mass spectrometry and a 12-point standard curve ranging from 0.01µg/mL up to 50µg/mL and weighted linear regression.

MALDI MSI was used to map the spatial distribution of CoQ10, related quinones, and metabolites. Tissue sections were cryosectioned at 10 µm and analyzed using a Bruker timsTOF flex instrument in negative ion mode at 20 µm pixel resolution. 1,5-Diaminonaphthalene (DAN) was applied as the matrix and (D9) CoQ10 internal standard was sprayed onto the sections for signal normalization.

## COQ BIOSYNTHETIC PATHWAY, SPATIAL QUINOMICS, AND PRIMARY COQ10 DEFICIENCY

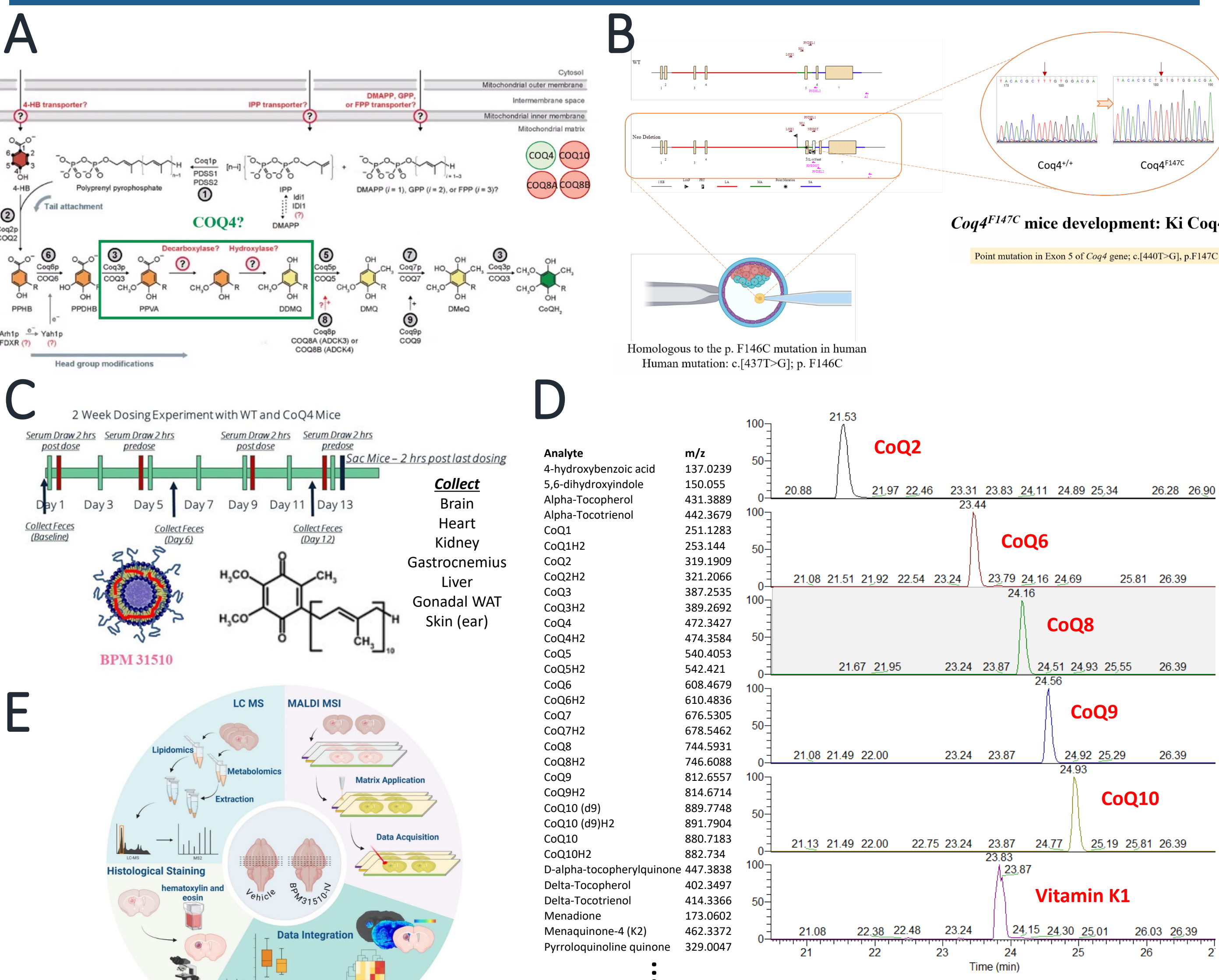


FIGURE LEGEND 1: CoQ10 biosynthetic pathway including the proposed function of COQ4, which together with other regulatory proteins maintain the CoQ pool (A). COQ4 KI genetic model (B). Study design treating WT and COQ4KI mice with BPM31510 over the course of two weeks of dosing to evaluate CoQ10 tissue distribution (C). LC MS/MS and spatial quinomics workflow (D) and (E).

## BPM31510 INCREASES TISSUE COQ10 LEVELS IN COQ4KI MOUSE MODEL

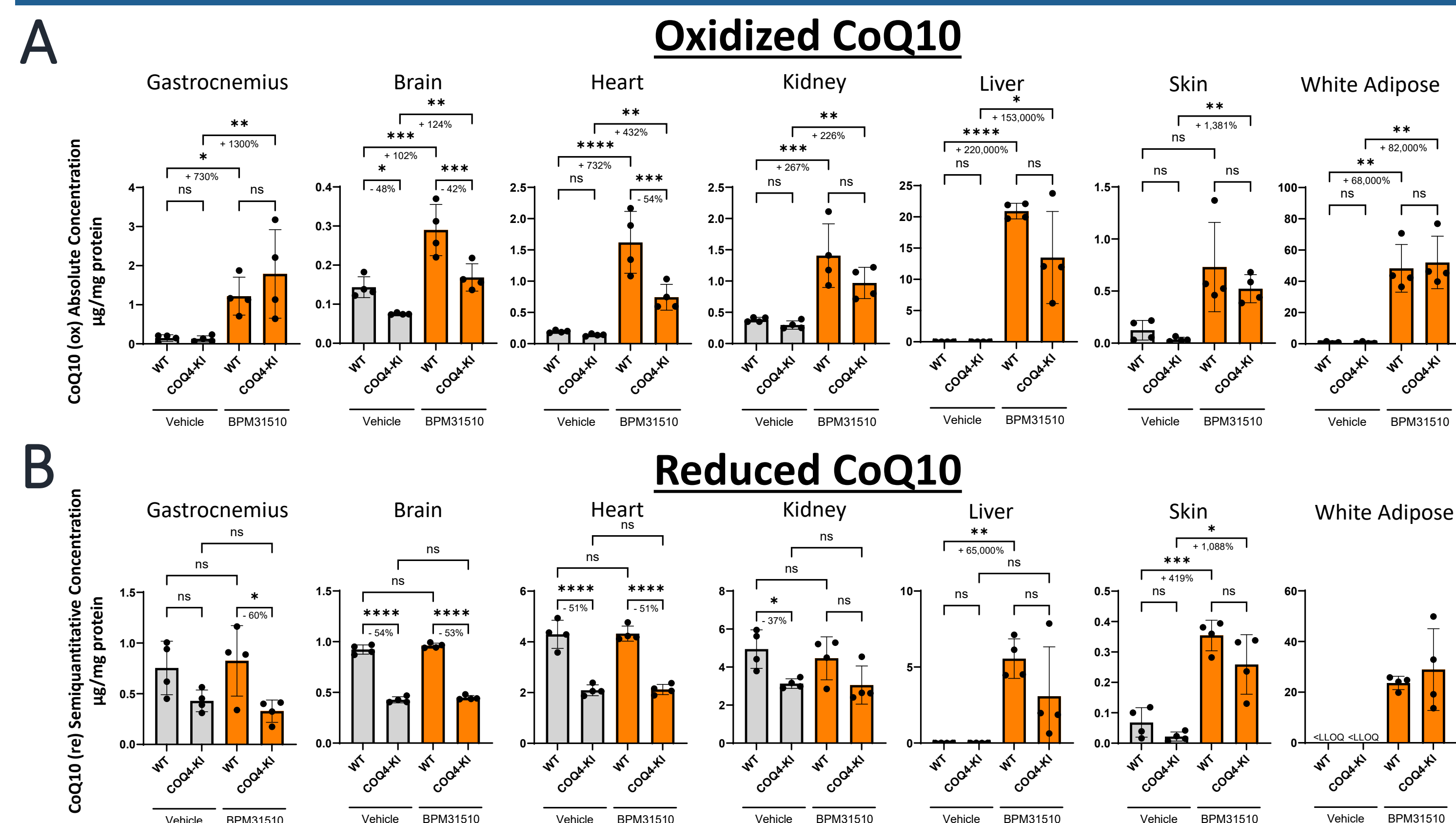


FIGURE LEGEND 2: Tissue CoQ10(oxidized) absolute concentrations (A), or CoQ10(reduced) semiquantitative concentrations (B) in WT and COQ4 KI mice, with or without BPM31510 treatment

## THE COQ POOL IS ENRICHED IN THE GASTROCNEMIUS FOLLOWING TREATMENT WITH BPM31510

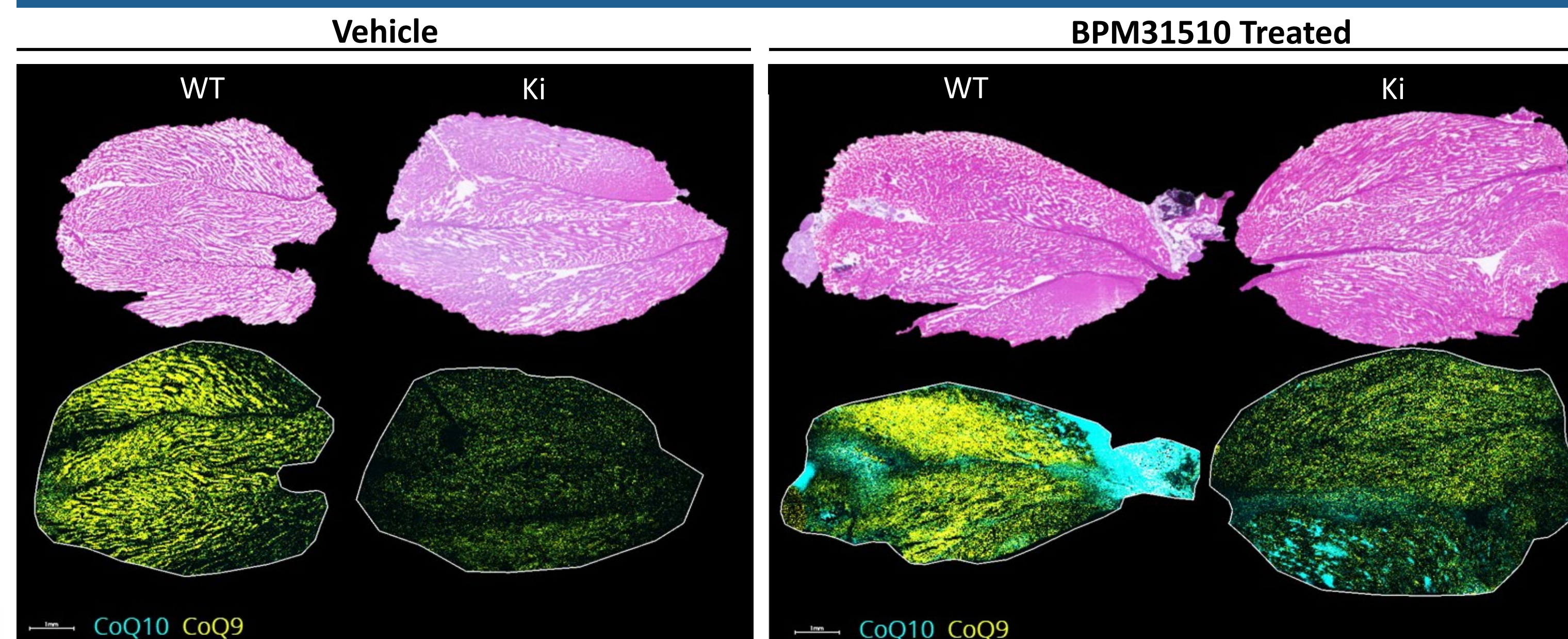


FIGURE LEGEND 3: Spatial assessment of CoQ9 and CoQ10 in WT and COQ4 KI vehicle and BPM31510 treated mice.

## BPM31510 DELIVERS COQ10 TO THE CEREBELLUM AND OTHER BRAIN REGIONS

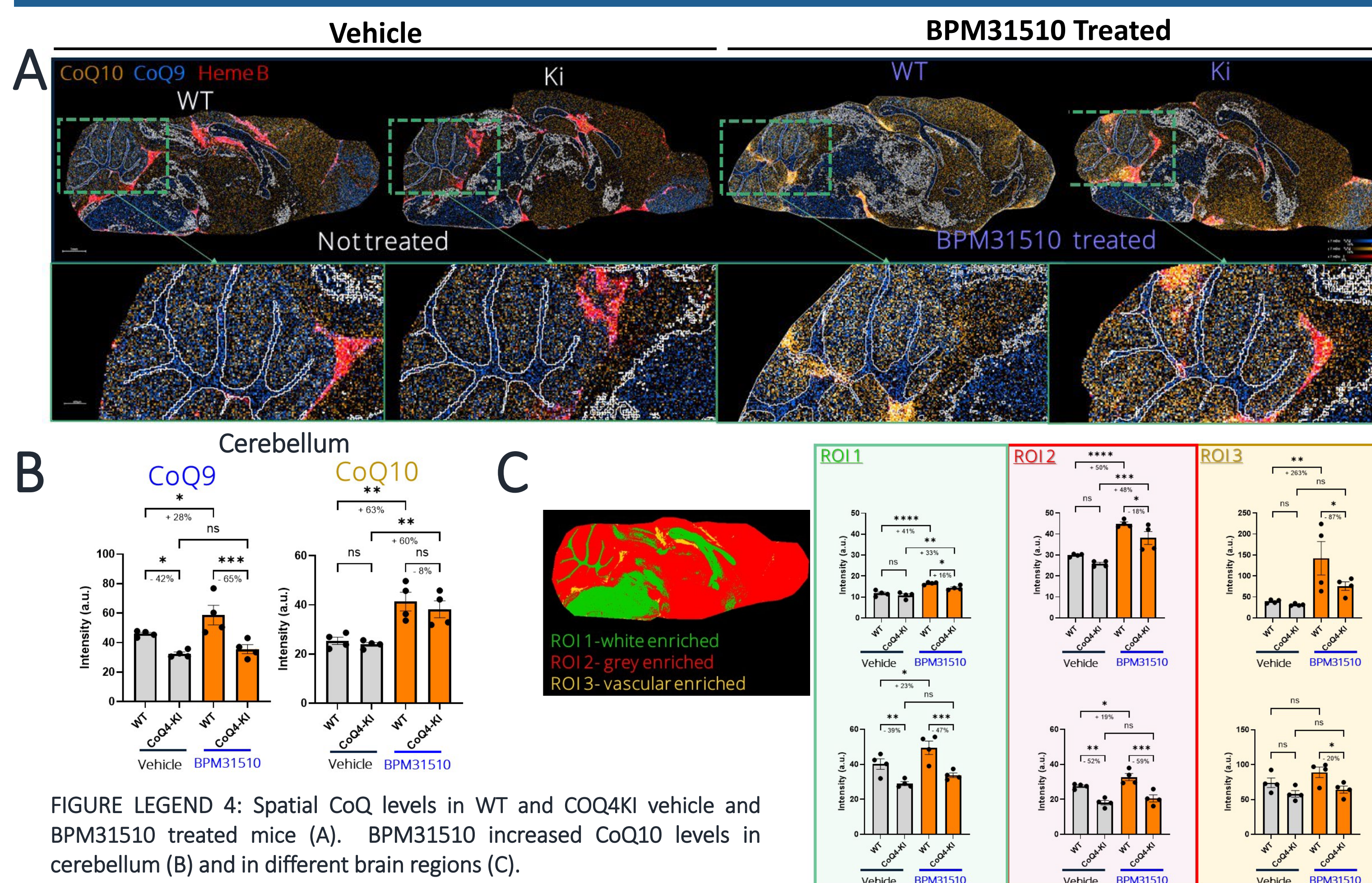


FIGURE LEGEND 4: Spatial CoQ levels in WT and COQ4KI vehicle and BPM31510 treated mice (A). BPM31510 increased CoQ10 levels in cerebellum (B) and in different brain regions (C).

## BPM31510 INCREASES COQ POOL IN KIDNEY

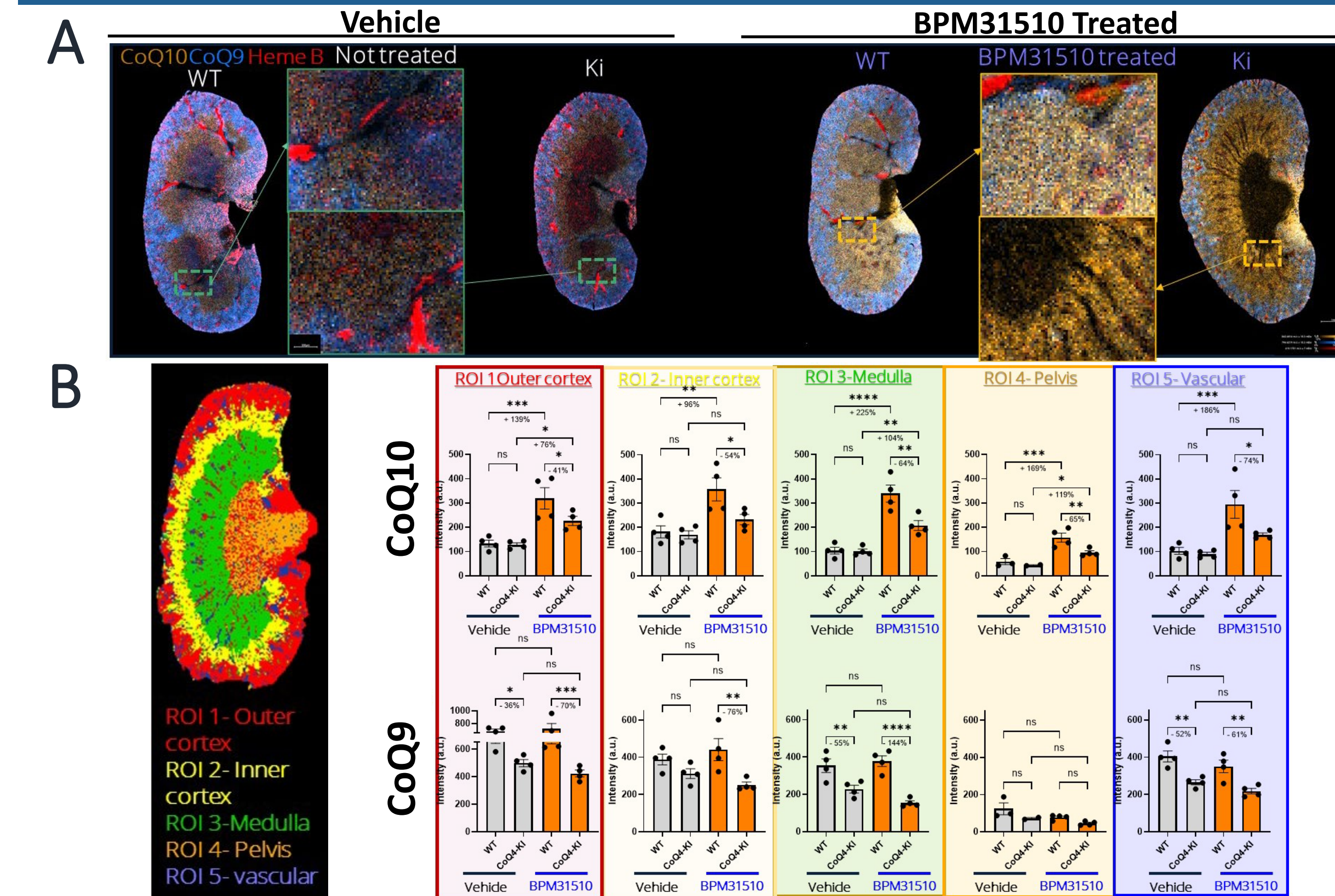


FIGURE LEGEND 5: Spatial resolution of CoQ9, CoQ10, and HEME B (marker for vascular system) in WT and COQ4KI vehicle or BPM31510 treated mice (A). Kidney segmentation analysis reveals kidney subregion CoQ9 deficiencies in COQ4KI compared to WT. BPM31510 treatment increased CoQ10 levels in WT and COQ4KI kidney subregions increasing the overall CoQ pool (B).

## CARDIAC COQ10 LEVELS INCREASE FOLLOWING TREATMENT WITH BPM31510

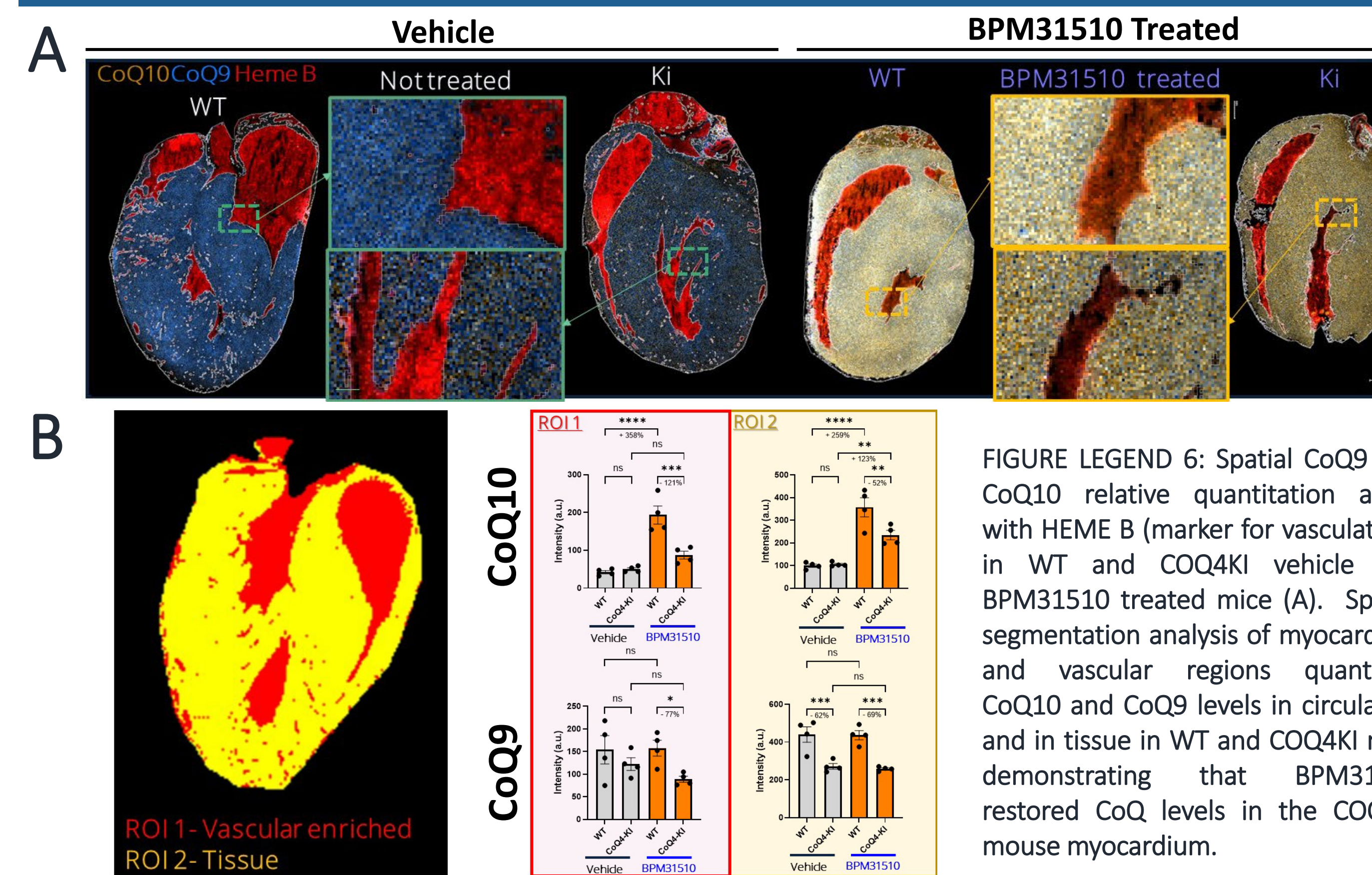


FIGURE LEGEND 6: Spatial CoQ9 and CoQ10 relative quantitation along with HEME B (marker for vasculature) in WT and COQ4KI vehicle and BPM31510 treated mice (A). Spatial segmentation analysis of myocardium and vascular regions quantified CoQ10 and CoQ9 levels in circulation and in tissue in WT and COQ4KI mice demonstrating that BPM31510 restored CoQ levels in the COQ4KI mouse myocardium.

## CONCLUSIONS

- Primary CoQ10 deficiency is a complex metabolic disorder in which LC MS/MS based quinomics and spatial quinomics approach offers novel insight into therapeutic development strategies
- Oral CoQ10 therapeutic approaches results in poor bioavailability, however, BPM31510 treatment has demonstrated enhanced bioavailability and tissue distribution.
- COQ4KI mouse model exhibits significant CoQ deficiencies in brain, heart and kidney, and BPM31510 was able to increase the CoQ pool through the increase of CoQ10 in these tissues.
- Brain delivery represents a predominant goal of therapeutic intervention in primary CoQ10 deficiency due to this disorder presenting with ataxia.
- In other tissues, such as muscle, heart, kidney, liver, skin and white adipose, BPM31510 significantly increased CoQ10 levels, demonstrating the enhanced tissue distribution and restoration of the CoQ pool.
- BPM31510 demonstrated significant CoQ10 delivery to an animal model of primary CoQ deficiency resulting in a restoration of CoQ, correcting the deficiency.